# Multi-task Prediction of Disease Onsets from Longitudinal Lab Tests

**Narges Razavian, Jake Marcus, David Sontag**
Courant Institute of Mathematical Sciences, New York University
{razavian,jmarcus,dsontag}@cs.nyu.edu

## Abstract

Disparate areas of machine learning have benefited from models that can take raw data with little preprocessing as input and learn rich representations of that raw data in order to perform well on a given prediction task. We evaluate this approach in healthcare by using longitudinal measurements of lab tests, one of the more raw signals of a patient's health state widely available in clinical data, to predict disease onsets. In particular, we train a Long Short-Term Memory (LSTM) recurrent neural network and two novel convolutional neural networks for multi-task prediction of disease onset for 133 conditions based on 18 common lab tests measured over time in a cohort of 298K patients derived from 8 years of administrative claims data. We compare the neural networks to a logistic regression with several hand-engineered, clinically relevant features. We find that the representation-based learning approaches significantly outperform this baseline. We believe that our work suggests a new avenue for patient risk stratification based solely on lab results.

## 1. Introduction

The recent success of deep learning in disparate areas of machine learning has driven a shift towards machine learning models that can learn rich, hierarchical representations of raw data with little preprocessing and away from models that require manual construction of features by experts (Graves and Schmidhuber, 2005; Krizhevsky et al., 2012; Mikolov et al., 2013). In natural language processing, for example, neural networks taking only character-level input achieve high performance on many tasks including text classification tasks (Zhang et al., 2015; Kim, 2014), machine translation (Ling et al., 2015) and language modeling (Kim et al., 2016).

Following these advances, attempts to learn features from raw medical signals have started to gain attention too. Lasko et al. (2013) studied a method based on sparse auto-encoders to learn temporal variation features from 30-day uric acid observations to distinguish between gout and leukemia. Che et al. (2015) developed a training method which, when datasets are small, allows prior domain knowledge to regularize the deeper layers of a feed-forward network for the task of multiple disease classification. Recent studies (Lipton et al., 2015; Choi et al., 2015) used Long Short-Term Memory (LSTM) recurrent neural networks (RNNs) for disease phenotyping.

In this paper, we evaluate the representation-based learning approach in healthcare by using longitudinal measurements of laboratory tests, one of the more raw signals of a

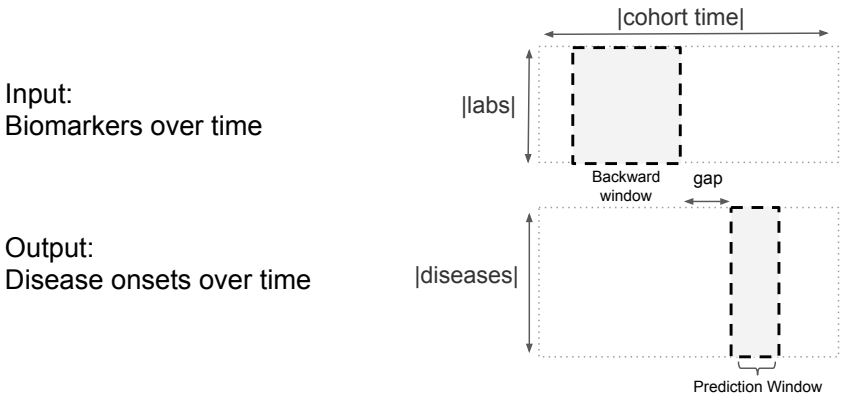


Figure 1: Overview of our prediction framework.

patient's health state widely available in clinical data, to predict disease onsets. We show that several multi-task neural networks, including a LSTM RNN and two novel convolutional neural networks, can aid in early diagnosis of a wide range of conditions (including conditions that the patient was not specifically tested for) without having to hand-engineer features for each condition. The source code of our implementation is available at `https://github.com/clinicalml/deepDiagnosis`.

## 2. Prediction Task

Figure 1 outlines the study's prediction framework. Our goal is early diagnosis of diseases for people who do not already have the disease. We required a 3-month gap between the end of the backward window, denoted $t$, and the start of the diagnosis window. The purpose of the 3 month gap was to ensure that the clinical tests taken right before the diagnosis of a disease would not allow our system to cheat in the prediction of that disease. Each output label was defined as positive if the diagnosis code for the disease was observed in at least 2 distinct months between 3 to $3+12$ months after $t$. Using 12 months helps alleviate the noisy label problem. Requiring at least 2 observations of the code also reduced the noise coming from physicians who report their wrong *suspected* diagnosis as a diagnosis. For each disease, we excluded individuals who already have the disease by time $t+3$. For exclusion, we required only 1 diagnosis record instead of 2 in order to remove patients who are even suspected of having the disease previously. This results in a more difficult, but more clinically meaningful prediction task.

Formally, we define the task of diagnosis as a supervised multi-task sequence classification problem. Each individual has a variable-length history of lab observations ($X$) and diagnosis records ($Y$). $X$ is continuous valued and $Y$ is binary. We use a sliding window framework to deal with variable length input. At each time point $t$ for each person, the model looks at a backward window of $B$ months of all $D$ biomarkers of the input, $X^{1:D}_{t-B:t}$, to predict the output. The output is a binary vector $Y$ of length $M$ indicating for each of the $M$ diseases whether they are newly diagnosed in the following months $t+3$ to $t+3+12$, where 3 is the *gap* and 12 is the *prediction window*.

## 3. Cohort

Our dataset consisted of lab measurement and diagnosis information for 298,000 individuals. The lab measurements had the resolution of 1 month and we used a backward window of 36 months for each prediction. These individuals were selected from a larger cohort of 4.1 million insurance subscribers between 2005 and 2013. We only included members who had at least one lab measurement per year for at least 3 consecutive years.

We used lab tests that comprise a comprehensive metabolic panel plus cholesterol and bilirubin (18 lab tests in total), which are currently recommended annually and covered by most insurance companies in the United States. The names and codes of the labs used in our analysis are included in the Supplementary Materials. Each lab value was normalized by subtracting its mean and dividing by the standard deviation computed across the entire dataset. We randomly divided individuals into a 100K training set, a 100K validation set, and a 98K test set. The validation set was used to select the best epoch/parameters for models and prediction results are presented on the test set unseen during training and validation.

The predicted labels corresponded to diagnosis information for these individuals. In our dataset, each disease diagnosis is recorded as an ICD9-CM (International Classification of Diseases, Ninth Revision, Clinical Modification) code.

## 4. Methods

We now describe the baseline model, the two novel convolutional (Le Cun et al., 1990; LeCun et al., 1998) architectures and the recurrent neural network with long short-term memory units (Hochreiter and Schmidhuber, 1997) that we evaluate on this prediction task. The input to the baseline model are hand-engineered features derived from the patient's lab measurements, whereas the input to the representation-based models are the raw, sparse and asynchronously measured lab measurements. We also report the results of an ensemble of the representation-based models.

### 4.1 Baseline

We trained a Logistic Regression model on a large set of features derived from the patient's lab measurements. These features included the minimum, maximum and latest observation value for each of the labs as well as binary indicators for increasing and decreasing trends in the lab values within the backward window. The continuous features were computed on lab values that were normalized across the cohort (to have zero mean and unit variance). We used the validate data to choose the type and amount of L1, L2, and Dropout (Srivastava et al., 2014) regularization, separately for each disease.

### 4.2 Multi-resolution Convolutional Neural Network (CNN1)

The architecture for our first convolutional neural network is shown in Figure 2. We define $X_{t-B:t}^{1:D}$ to be the input to the network at time $t$ for $D$ lab measurements over the past $B$ months. Let $J$ be the number of filters in each convolution operator. Each filter $K_i^j$ $(j = 1 : J)$ is of size $1 \times L$. The output of the convolution part of the network is a vector

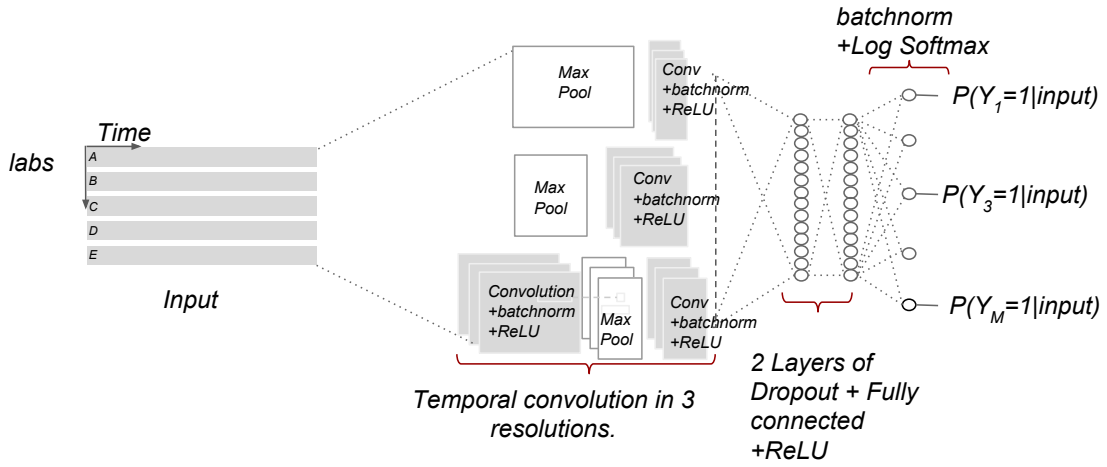


Figure 2: Architecture for Multi-resolution Convolutional Neural Network (CNN1)

$C = [C_1, C_2, C_5]$ which is defined as follows:

$$C_1^{d,j} = f(b_1^j + K_1^j * \text{MaxPool}(X_{t-B:t}^d, p^2)) \quad (1)$$

$$C_2^{d,j} = f(b_2^j + K_2^j * \text{MaxPool}(X_{t-B:t}^d, p)) \quad (2)$$

$$C_3^{d,j} = f(b_3^j + K_3^j * X_{t-B:t}^{1:D}) \quad (3)$$

$$C_4^{d,j} = \text{MaxPool}(C_3^{d,j}, p) \quad (4)$$

$$C_5^{d,j} = f(b_5^j + \sum_{k=1}^{J} K_5^j * C_4^{d,k}) \quad (5)$$

In the equations above, the nonlinearity $f$ is a rectified linear unit (ReLU) (Nair and Hinton, 2010) applied element-wise to a vector, and $*$ is the standard convolution operation. $\text{MaxPool}(Z, s)$ corresponds to a non-overlapping max pooling operation with step size $k$, defined as $\text{MaxPool}(Z, s)[i] = \max(Z_{i \cdot s}, \ldots, Z_{(i+1) \cdot s - 1})$ for $i = 1 : \lfloor \text{length}(Z)/s \rfloor$. We set $p = 3$ for this paper. The vector $C_i$ is the concatenation of $C_i^{d,j}$ for all labs $d = 1 : D$ and filters $j = 1 : J$. The outputs of the first and second level in the multi-resolution network, $(C_1, C_2)$, are results of the convolution operator applied to kernels $K_1^j$ and $K_2^j$ at different resolutions of the input. The third level of resolution includes two layers of convolution using filters $K_3^j$ and $K_5^j$. After every convolution operation, we use batch normalization (Ioffe and Szegedy, 2015).

After the multi-resolution convolution is applied, the vector $C = [C_1, C_2, C_5]$ represents the application of filters to all labs (note that the filters are shared across all the labs). We then use 2 layers of hidden nodes to allow non-linear combination of filter activations on different labs:

$$h_1 = f(W_1^T C + b_{h_1}) \quad (6)$$

$$h_2 = f(W_2^T h_1 + b_{h_2}) \quad (7)$$

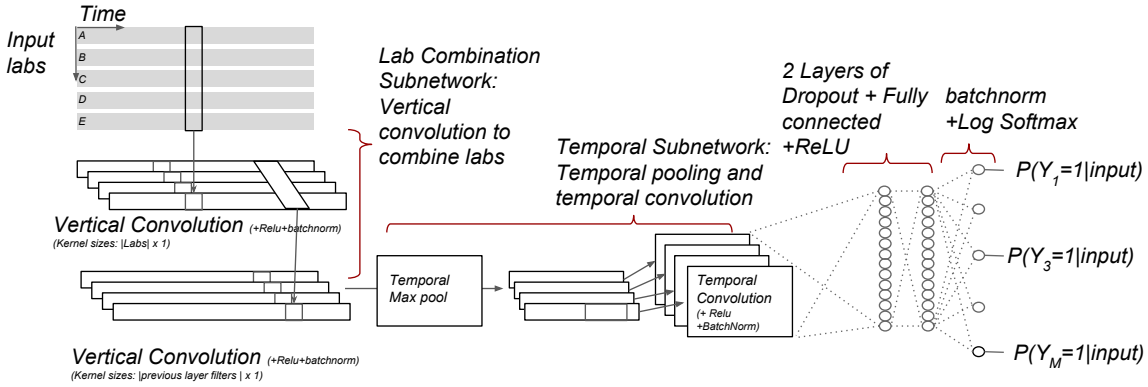


Figure 3: Architecture for Convolutional Neural Network over Time and Input dimensions (CNN2)

$W_i$ are the weights for the hidden nodes and $b_{h_i}$ is the bias associated with each layer. Each of the hidden layers are subject to Dropout regularization (with probability 0.5) during training, and are followed by batch normalization.

Finally, for each disease $m = 1 : M$, the model predicts the likelihood of the disease via logistic regression over $h_2$:

$$P(Y_m = 1|X^{1:D}_{t-B:t}) = \sigma(W_m^T h_2 + b_m), \tag{8}$$

where $\sigma(x) = 1/(1 + e^{-x})$ is the sigmoid function. The loss function for each disease is the negative log likelihood of the true label, weighted by the inverse-label frequency to handle class imbalance during multi-task batch training. Diseases are trained independently, but the gradient is backpropagated through the shared part of the network for all diseases.

### 4.3 Convolutional Neural Network over Time and Input dimensions (CNN2)

The architecture for our second convolutional neural network is shown in Figure 3. In this model, we first combine the labs via a vertical convolution with kernels that span across all labs. Having a few such combination layers enables us to project from the lab space into a new latent space which might better encode information about the labs. We then focus on temporal encoding of the result in the new space.

Given the input $X^{1:D}_{t-B:t}$, the output of the first vertical convolution with $L$ filters $K^{1:L}$, each of size $(D \times 1)$, and nonlinearity $f$ is $V^{t-B:t}_{1:L}$ of size $(L \times 1 \times B)$, where

$$V^{t-B:t}_l = f(b_l + K^l * X^{1:D}_{t-B:t}) \tag{9}$$

for $l = 1 : L$. We then repeat, applying new convolution filters of size $L \times 1$ to $V^{t-B:t}_{1:L}$, followed again by a nonlinearity $f$ (ReLU in our experiments), giving us two hidden layers in the vertical direction. Finally, temporal max pooling and convolution is applied to the last convolution output followed by two fully connected layers, similar to equations (2) and (6) through (8). Similar to the previous architecture, we optimize the weighted negative log-likelihood of the disease labels on the training data.

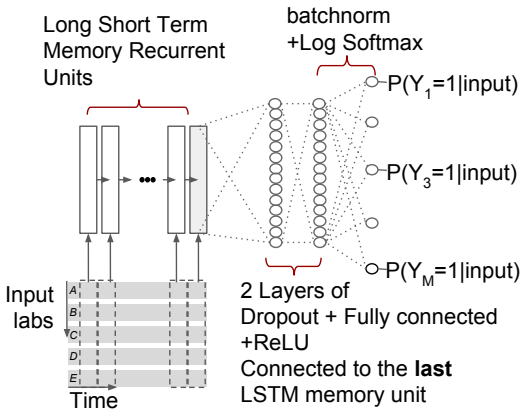


Figure 4: Architecture for the Long Short-Term Memory Network (LSTM)

### 4.4 Long Short-Term Memory Network (LSTM)

The architecture for the Recurrent Neural Network with Long Short-Term Memory units (Hochreiter and Schmidhuber, 1997) is shown in Figure 4. These models encode a memory state $c_{\hat{t}}$ at each time step $\hat{t}$, which is only accessible through a particular gating mechanism. Given input $X_{\hat{t}}$ and the output and memory state of the recurrent network at time $\hat{t}-1$ ($h_{\hat{t}-1}$), the memory state and output for time steps $\hat{t}:t-B:t$ are computed as follows:

$$i_{\hat{t}} = \sigma(W_{x\to i}X_{\hat{t}} + W_{h\to i}h_{\hat{t}-1} + W_{c\to i}c_{\hat{t}-1} + b_{1\to i}) \tag{10}$$

$$f_{\hat{t}} = \sigma(W_{x\to f}X_{\hat{t}} + W_{h\to f}h_{\hat{t}-1} + W_{c\to f}c_{\hat{t}-1} + b_{1\to f}) \tag{11}$$

$$z_{\hat{t}} = \tanh(W_{x\to c}X_{\hat{t}} + W_{h\to c}h_{\hat{t}-1} + b_{1\to c}) \tag{12}$$

$$c_{\hat{t}} = f_{\hat{t}}c_{\hat{t}1} + i_{\hat{t}}z_{\hat{t}} \tag{13}$$

$$o_{\hat{t}} = \sigma(W_{x\to o}X_{\hat{t}} + W_{h\to o}h_{\hat{t}-1} + W_{c\to o}c_{\hat{t}} + b_{1\to o}) \tag{14}$$

$$h_{\hat{t}} = o_{\hat{t}}\tanh(c_{\hat{t}}) \tag{15}$$

where $W_*$ and $b_*$ are the network's parameters, shared across all time steps. We use the output of the last time point, $h_t$, as the patient representation (i.e. $C$ in Eq. (6)). The rest of the network is the same as described in Eq. (6) through (8) and we minimize the weighted negative log-likelihood.

### 4.5 Weighted Batch Training to Deal with Class Imbalance

We observed in our initial experiments that the predictive performance for more common diseases converges faster than for the uncommon diseases. Since early stopping is so important for preventing overfitting in neural networks, this leads to the following dilemma: either we stop early and underfit for the less common diseases, or we continue learning and overfit for the more common diseases. Decoupling them is not possible because of the shared patient representation. To alleviate this problem and following Firat et al. (2016), we use a weighted negative log-likelihood as the loss function. Specifically, we weight the gradient coming from each disease by the frequency of that disease. Our experiments indicated that the weighting improves the overall prediction results.

## 5. Results

We used the validation set of 100K individuals to fine tune the hyperparameters of all our models. We then evaluated the best models on a test set of size 98K individuals. We describe the details of the architectures chosen in the Supplementary Materials. We report the Area Under the ROC curve (AUC) on the test set. We implemented these experiments in Torch (Collobert et al., 2011). The source code of our implementation is available at `https://github.com/clinicalml/deepDiagnosis`.

Table 1 shows the AUC results for the top 25 diseases sorted by the maximum AUC that any model achieved on the test set. An ensemble of the neural networks performed best followed by the CNN2 architecture. The neural networks consistently outperformed the baseline in predicting the new onset of diseases 3 months in advance. In particular, heart failure, severe kidney diseases and liver problems, diabetes and hormone related conditions, and prostate cancer are among the diseases most accurately detected early from only 18 common lab measurements tracked over the previous 3 years. Our proposed models improve the quality of prediction for prostate cancer, elevated prostate specific antigen (note that the PSA lab is not part of our input), breast cancer, colon cancer, macular degeneration, and congestive heart failure most strongly. In the Supplementary Materials, we also report the top features from the baseline model for several of the diseases.

## 6. Case study: Chronic Kidney Disease Progression

We adapted the multitask architecture to predict the onset of end-stage renal disease (ESRD) requiring dialysis or a kidney transplant based on labs related to kidney function as well as diagnoses and prescriptions in a cohort of patients with advanced chronic kidney disease (CKD).

Predictive models for ESRD in patients with advanced kidney disease could improve the timeliness of referral to a nephrologist enabling, for example, early counseling and education for high risk patients before they start dialysis (Green et al., 2012). Clinical guidelines recommend that patients be referred to a nephrologist at least one year before they might be anticipated to require dialysis, and late referral may result in more rapid progression to kidney failure, worse quality of life for patients on dialysis, and missed opportunities for pre-emptive kidney transplantation (UK-Renal-Assocation, 2014).

See Echouffo-Tcheugui and Kengne (2012) for a review of the literature on risk models for CKD. More recently, Hagar et al. (2014) undertook a survival analysis for the progression of CKD using electronic health record data, Perotte et al. (2015) developed a risk model to predict progression from Stage 3 to Stage 4 CKD, and Fraccaro et al. (2016) evaluated several risk models for predicting the onset of CKD.

### 6.1 Data and Experiments Setup

We use the same dataset as in the multi-disease prediction task. We restrict our analysis to patients with Stage 4 CKD, which we define as patients with at least 2 measurements of the estimated Glomerular Filtration Rate (eGFR) between 15 and 30 mL/min/1.73m$^2$ observed at least 90 days apart (KDIGO, 2012). We exclude patients with very sparse lab data by

| ICD9 Code and disease description | **LR** | **LSTM** | **CNN1** | **CNN2** | **Ens** | **Pos** |
|---|---|---|---|---|---|---|
| 585.6 End stage renal disease | 0.886 | 0.917 | 0.910 | 0.916 | 0.920 | 837 |
| 285.21 Anemia in chr kidney dis | 0.849 | 0.866 | 0.868 | 0.880 | 0.879 | 1598 |
| 585.3 Chr kidney dis stage III | 0.846 | 0.851 | 0.857 | 0.858 | 0.864 | 2685 |
| 584.9 Acute kidney failure NOS | 0.805 | 0.820 | 0.828 | 0.831 | 0.835 | 3039 |
| 250.01 DMI wo cmp nt st uncntrl | 0.822 | 0.813 | 0.819 | 0.825 | 0.829 | 1522 |
| 250.02 DMII wo cmp uncntrld | 0.814 | 0.819 | 0.814 | 0.821 | 0.828 | 3519 |
| 593.9 Renal and ureteral dis NOS | 0.757 | 0.794 | 0.784 | 0.792 | 0.798 | 2111 |
| **428.0 CHF NOS** | 0.739 | 0.784 | 0.786 | 0.783 | 0.792 | 3479 |
| V053 Need prphyl vc vrl hepat | 0.731 | 0.762 | 0.752 | 0.780 | 0.777 | 862 |
| **790.93 Elvtd prstate spcf antgn** | 0.666 | 0.758 | 0.761 | 0.768 | 0.772 | 1477 |
| **185 Malign neopl prostate** | 0.627 | 0.757 | 0.751 | 0.761 | 0.768 | 761 |
| 274.9 Gout NOS | 0.746 | 0.761 | 0.764 | 0.757 | 0.767 | 1529 |
| **362.52 Exudative macular degen** | 0.687 | 0.752 | 0.750 | 0.757 | 0.765 | 538 |
| **607.84 Impotence, organic orign** | 0.663 | 0.739 | 0.736 | 0.748 | 0.752 | 1372 |
| 511.9 Pleural effusion NOS | 0.708 | 0.736 | 0.742 | 0.746 | 0.749 | 2701 |
| **616.10 Vaginitis NOS** | 0.692 | 0.736 | 0.736 | 0.746 | 0.747 | 440 |
| **600.01 BPH w urinary obs/LUTS** | 0.648 | 0.737 | 0.737 | 0.738 | 0.747 | 1681 |
| **285.29 Anemia-other chronic dis** | 0.672 | 0.713 | 0.725 | 0.746 | 0.739 | 1075 |
| **346.90 Migrne unsp wo ntrc mgrn** | 0.633 | 0.736 | 0.710 | 0.724 | 0.732 | 471 |
| 427.31 Atrial fibrillation | 0.687 | 0.725 | 0.728 | 0.733 | 0.736 | 3766 |
| 250.00 DMII wo cmp nt st uncntr | 0.708 | 0.718 | 0.708 | 0.719 | 0.728 | 3125 |
| 425.4 Prim cardiomyopathy NEC | 0.683 | 0.718 | 0.719 | 0.722 | 0.726 | 1414 |
| 728.87 Muscle weakness-general | 0.683 | 0.704 | 0.718 | 0.722 | 0.723 | 4706 |
| **620.2 Ovarian cyst NEC/NOS** | 0.660 | 0.720 | 0.700 | 0.711 | 0.719 | 498 |
| 286.9 Coagulat defect NEC/NOS | 0.690 | 0.694 | 0.709 | 0.715 | 0.718 | 958 |

Table 1: AUC results on the test set for different models for the top 25 diseases sorted by maximum AUC achieved by any of the models. Bold indicates that proposed models improve AUC by at least 0.05 compared to the baseline with hand-engineered features. Abbreviations: LR = Logistic Regression. CNN1 = Convolutional neural network architecture 1 (Figure 2). CNN2 = Convolution neural network architecture 2 (Figure 3). LSTM = Long Short-Term Memory Network (Figure 4). Ens = Ensemble of the deep models. Pos = Number of positive examples in the test set.

requiring at least one measurement of eGFR every 4 months of the training window. NICE (2014) recommends 2-3 measurements of eGFR a year for patients with Stage 4 CKD.

We formulate the prediction task as taking a year of a patient's lab, diagnosis, prescription and demographic data as input and outputting a guess for whether or not that patient will start dialysis or undergo a kidney transplantation at any point in a 1-year window starting 3 months after the end of that year of clinical data. A training example for this prediction task consists of a matrix $X$ for a patient-year with $X[i, j]$ = the value of the $i$th clinical or demographic feature (the average value for each lab, an indicator for each ICD9 code and drug class prescription, an indicator for gender and a continuous value for age)

for the patient in the $j$th month of the year and an indicator $Y$ with $Y = 1$ if the patient starts dialysis or undergoes a kidney transplantation in the 1-year outcome window and 0 otherwise.

We included the labs associated with the most common LOINC codes for all of the labs used in the predictive models for kidney failure developed by Tangri et al. (2011) and the labs with high prevalence in the CKD cohort analyzed by Hagar et al. (2014). We also included drug classes common in the treatment of kidney disease (HealthPartners-Kidney-Health-Clinic, 2011) and ICD9 codes with high mutual information comparing positive to negative examples on the training data (withholding the validation and test data). Table 3 shows the final list of clinical features.

For each patient in the cohort, we obtain multiple training examples by constructing an $X$ for the one-year period starting at the 1st observation of eGFR for that patient, another $X$ for the one-year period starting at the 2nd observation of eGFR for that patient, and so on for every observation of eGFR in the patient's record. We exclude training examples where a dialysis CPT code appears before the start of the 1-year outcome window.

This process results in 29,937 examples (5,484 patients) with 2,619 positive examples (781 patients). We randomly divide these patients into 3 roughly equal groups and assign all the examples for a patient to the training, validation or test dataset.

Figure 5 in the Supplementary Materials shows an example of lab data for a patient that does not start dialysis or undergo a kidney transplant in the outcome window and for a patient the starts dialysis in the outcome window.

We compared the performance of the CNN2 architecture adapted to this prediction task to two logistic regression baselines and a random forest. Additional details are provided in the Supplementary Materials.

### 6.2 Results

The 4 models achieved similar performance on this prediction task (see Table 4). The small sample size and the single binary outcome distinguish this task from the multi-disease setting and may make it difficult to observe large differences in performance between the models. A small number of features also seem to account for much of the signal. We observed that a logistic regression with a large L1 penalty achieves good performance on the task despite only using eGFR, urea nitrogen, age and gender as features.

## 7. Conclusion

In this work, we presented a large-scale application of two novel convolutional neural network architectures and a LSTM recurrent neural network for the task of multi-task early disease onset detection. These representation-based approaches significantly outperform a logistic regression with several hand-engineered, clinically relevant features. Interestingly, in our earlier work, we found that despite the large amount of missing data in the setting considered, preprocessing the data by imputing missing values did not significantly improve results (Razavian and Sontag, 2015). As medical home and consumer healthcare technologies rapidly progress, we envision a growing role for automatic risk stratification of patients based solely on raw physiological and chemical signals.

## Acknowledgments

The authors gratefully acknowledge support by Independence Blue Cross. The Tesla K40s used for this research were donated by the NVIDIA Corporation. We thank Dr. Yindalon Aphinyanaphongs, Dr. Steven Horng, and Dr. Saul Blecker for providing helpful clinical perspectives throughout this research.

## References

J Bergstra and Y Bengio. Random search for hyper-parameter optimization. *Journal of Machine Learning Research*, 2012.

Zhengping Che, David Kale, Wenzhe Li, Mohammad Taha Bahadori, and Yan Liu. Deep computational phenotyping. In *Proceedings of the 21th ACM SIGKDD International Conference on Knowledge Discovery and Data Mining*, pages 507–516. ACM, 2015.

Edward Choi, Mohammad Taha Bahadori, and Jimeng Sun. Doctor ai: Predicting clinical events via recurrent neural networks. *arXiv preprint arXiv:1511.05942*, 2015.

Ronan Collobert, Koray Kavukcuoglu, and Clément Farabet. Torch7: A matlab-like environment for machine learning. In *BigLearn, NIPS Workshop*, number EPFL-CONF-192376, 2011.

JB Echouffo-Tcheugui and AP Kengne. Risk models to predict chronic kidney disease and its progression: a systematic review. *PLoS Medicine*, 2012.

Orhan Firat, Kyunghyun Cho, and Yoshua Bengio. Multi-way, multilingual neural machine translation with a shared attention mechanism. *arXiv preprint arXiv:1601.01073*, 2016.

Pablo Fraccaro, Sabine van der Veer, Benjamin Brown, Mattia Prosperi, Donal O'Donoghue, Gary Collins, Iain Buchan, and Niels Peek. Risk prediction for chronic kidney disease progression using heterogeneous electronic health record data and time series analysis. *BMC Medicine*, 2016.

Alex Graves and Jürgen Schmidhuber. Framewise phoneme classification with bidirectional lstm and other neural network architectures. volume 18, pages 602–610. Elsevier, 2005.

D Green, J Ritchie, D New, and Kalra P. How accurately do nephrologists predict the need for dialysis within one year? *Nephron Clin Practice*, 2012.

Y Hagar, DJ Albers, R Pivovarov, HS Chase, V Dukic, and N Elhadad. Survival analysis adapted for electronic health record data: Experiments with chronic kidney disease. *Statistical Analysis and Data Mining*, 2014.

HealthPartners-Kidney-Health-Clinic. Medications commonly used in chronic kidney disease. `https://www.healthpartners.com/ucm/groups/public/@hp/@public/documents/documents/cntrb_010921.pdf`, 2011. Accessed: 8/1/16.

Sepp Hochreiter and Jürgen Schmidhuber. Long short-term memory. *Neural computation*, 9(8):1735–1780, 1997.

Sergey Ioffe and Christian Szegedy. Batch normalization: Accelerating deep network training by reducing internal covariate shift. *arXiv preprint arXiv:1502.03167*, 2015.

KDIGO. Kdigo 2012 clinical practice guideline for the evaluation and management of chronic kidney disease. `http://www.kdigo.org/clinical_practice_guidelines/pdf/CKD/KDIGO_2012_CKD_GL.pdf`, 2012. Accessed: 7/31/16.

Yoon Kim. Convolutional neural networks for sentence classification. *EMNLP*, 2014.

Yoon Kim, Yacine Jernite, David Sontag, and Alexander M Rush. Character-aware neural language models. In *Thirtieth AAAI Conference on Artificial Intelligence*, 2016.

Alex Krizhevsky, Ilya Sutskever, and Geoffrey E Hinton. Imagenet classification with deep convolutional neural networks. In *Advances in neural information processing systems*, pages 1097–1105, 2012.

Thomas A Lasko, Joshua C Denny, and Mia A Levy. Computational phenotype discovery using unsupervised feature learning over noisy, sparse, and irregular clinical data. volume 8, page e66341. Public Library of Science, 2013.

B Boser Le Cun, John S Denker, D Henderson, Richard E Howard, W Hubbard, and Lawrence D Jackel. Handwritten digit recognition with a back-propagation network. In *Advances in neural information processing systems*. Citeseer, 1990.

Yann LeCun, Léon Bottou, Yoshua Bengio, and Patrick Haffner. Gradient-based learning applied to document recognition. volume 86, pages 2278–2324. IEEE, 1998.

Wang Ling, Isabel Trancoso, Chris Dyer, and Alan W Black. Character-based neural machine translation. *arXiv preprint arXiv:1511.04586*, 2015.

Zachary C Lipton, David C Kale, Charles Elkan, and Randall Wetzell. Learning to diagnose with lstm recurrent neural networks. *arXiv preprint arXiv:1511.03677*, 2015.

Tomas Mikolov, Ilya Sutskever, Kai Chen, Greg S Corrado, and Jeff Dean. Distributed representations of words and phrases and their compositionality. In *Advances in neural information processing systems*, pages 3111–3119, 2013.

Vinod Nair and Geoffrey E Hinton. Rectified linear units improve restricted boltzmann machines. In *Proceedings of the 27th International Conference on Machine Learning (ICML-10)*, pages 807–814, 2010.

NICE. Chronic kidney disease in adults: assessment and management. `https://www.nice.org.uk/guidance/cg182/`, 2014. Accessed: 8/1/16.

A Perotte, R Ranganath, JS Hirsch, D Blei, and N Elhadad. Risk prediction for chronic kidney disease progression using heterogeneous electronic health record data and time series analysis. *JAMIA*, 2015.

Narges Razavian and David Sontag. Temporal convolutional neural networks for diagnosis from lab tests. *arXiv:1511.07938*, 2015.

Nitish Srivastava, Geoffrey Hinton, Alex Krizhevsky, Ilya Sutskever, and Ruslan Salakhutdinov. Dropout: A simple way to prevent neural networks from overfitting. volume 15, pages 1929–1958. JMLR, 2014.

N Tangri, L Stevens, J Griffith, H Tighiouart, O Djurdjev, D Naimark, A Levin, and A Levey. A predictive model for progression of chronic kidney disease to kidney failure. *JAMA*, 2011.

UK-Renal-Assocation. Uk renal assocation planning, initiating and withdrawal of renal replacement therapy. `http://www.renal.org/guidelines/modules/planning-initiating-and-withdrawal-of-renal-replacement-therapy#sthash.y62zbp1w.hwwtAiRh.dpbs`, 2014. Accessed: 8/1/16.

Matthew D Zeiler. Adadelta: an adaptive learning rate method. *arXiv preprint arXiv:1212.5701*, 2012.

Xiang Zhang, Junbo Zhao, and Yann LeCun. Character-level convolutional networks for text classification. In *Advances in Neural Information Processing Systems*, pages 649–657, 2015.

## 8. Supplementary Materials for Multi-task Prediction of Disease Onsets from Longitudinal Lab Tests

### 8.1 Cross-validation results

For the convolutional models, we set the number of filters to be 64 for all the convolution layers with a kernel length of 8 (months) and a step size of 1. Each max-pooling module had a horizontal length of 3 and vertical length of 1 with a step size of 3 in the horizontal direction (i.e. no overlap). Each convolution module was followed by a batch normalization module (Ioffe and Szegedy (2015)) and then a ReLU nonlinearity (Nair and Hinton (2010)). We had 2 fully connected layers (with 100 nodes each, cross validated over [30,50, 100, 500,1000]) after concatenating the outputs of all the convolution layers. Each of the fully connected layers were followed by a batch normalization layer and a ReLU nonlinearity layer. We also added one Dropout module (Srivastava et al. (2014)) (0.5 dropout probability) before each fully connected layer. We tested models with and without batch-normalization and found that the networks converge much faster with batch-normalization.

We had the following layers after the last ReLu nonlinearity for each of the 171 diseases: a Dropout layer(0.5 dropout probability), a fully connected layer (of size 2 nodes corresponding to binary outcome), a batch normalization layer and a Log Softmax Layer. A learning rate of 0.1 was selected from among the values $[0.001, 0.01, 0.05, 0.1, 1]$ using the validation set average AUC (over all diseases) after 10 epochs. Training was done using Adadelta(Zeiler (2012)) optimization, which is a variant of stochastic gradient descent with adaptive step size. We used mini-batches of size 256.

For the LSTM network, we cross-validated over the hidden LSTM units ([100 500 1000]), and 500 was selected as the best. For the shared part of the network, we used the best parameters found for the convolution models.

### 8.2 Model details for CKD Case Study

We compared the following models:

- CNN2. We applied the CNN2 architecture used in the multi-disease prediction task with 8 filters with kernel dimensions of 8x1. We used the raw clinical and demographic data as input without additional feature engineering. We chose the learning rate and the architecture based on cross-validation using random sampling of hyperparameters (Bergstra and Bengio (2012)).

- L2-regularized, logistic regression. For each lab, we added one feature for the average lab value across the training window. We included gender and the diagnosis and prescription data as binary indicators and age as a continuous variable. We chose a regularization constant based on cross-validation.

- L1-regularized, logistic regression. For each lab, we added features to the regression for the average lab value for the patient over the last 3 months of the training window, the past 6 months of the training window and over the entire training window. We also added binary features for whether or not the lab increased, decreased or fluctuated over the last 3 months, 6 months and over the entire training window. We included

Table 2: Name and LOINC of labs included as features for multi-task prediction

| Lab name | LOINC |
|---|---|
| Creatinine | 2160-0 |
| Urea nitrogen | 3094-0 |
| Potassium | 2823-3 |
| Glucose | 2345-7 |
| Alanine aminotransferase | 1742-6 |
| Aspartate aminotransferase | 1920-8 |
| Protein | 2885-2 |
| Albumin | 1751-7 |
| Cholesterol | 2093-3 |
| Triglyceride | 2571-8 |
| Cholesterol.in LDL | 13457-7 |
| Calcium | 17861-6 |
| Sodium | 2951-2 |
| Chloride | 2075-0 |
| Carbon dioxide | 2028-9 |
| Urea nitrogen/Creatinine | 3097-3 |
| Bilirubin | 1975-2 |
| Albumin/Globulin | 1759-0 |

gender and the diagnosis and prescription data as binary indicators and age as a continuous variable. We chose a regularization constant based on cross-validation.

- Random forests. We used the raw clinical and demographic data as input without additional feature engineering. We chose the number of trees in the forest, the maximum depth of each tree, the maximum number of features to consider when looking for the best split, the minimum number of samples required to split a node, and the minimum number of samples in newly created leaves based on cross-validation using random sampling of hyperparameters.

### 8.3 Figures and Tables

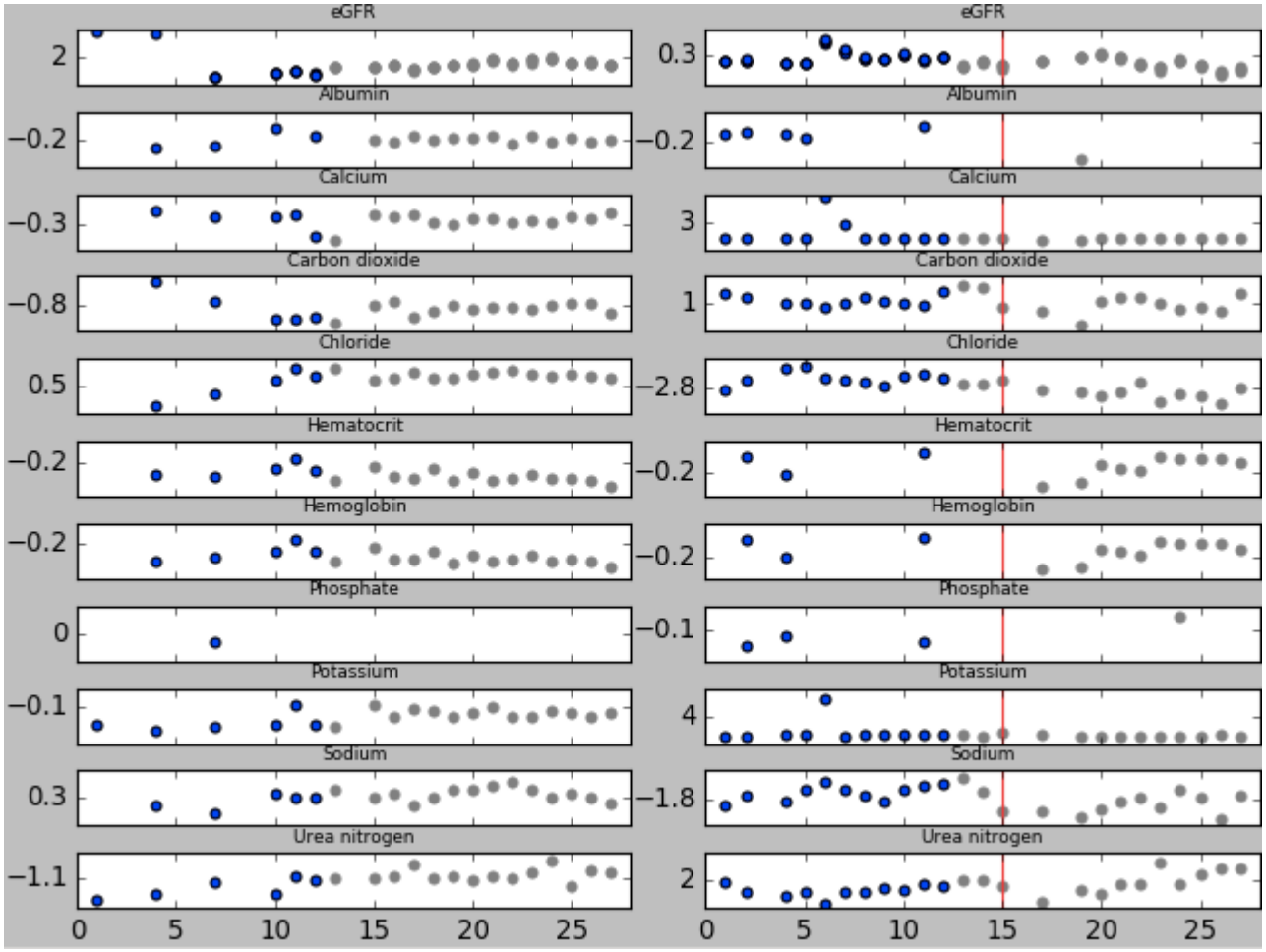


Figure 5: Monthly average lab values for two patients. The left pane show the lab data for a patient who doesn't initiate dialysis or undergo a kidney transplant. The right pane shows a patient that starts dialysis in the outcome window. The vertical red line shows when that patient starts dialysis. The x-axis is the number of months from the beginning of the training window and the y-axis is the standardized lab value.

Table 3: Clinical features included in predictive models in the CKD case study

| Type | Description |
|---|---|
| Lab | 33914-3 eGFR/1.73 sq M [Volume Rate/Area] in Serum or Plasma |
| Lab | 48642-3 eGFR/1.73 sq M among non-blacks [Volume Rate/Area] in Serum or Plasma |
| Lab | 48643-1 eGFR/1.73 sq M among blacks [Volume Rate/Area] in Serum or Plasma |
| Lab | 2160-0 Creatinine [Mass/volume] in Serum or Plasma |
| Lab | 1751-7 Albumin [Mass/volume] in Serum or Plasma |
| Lab | 17861-6 Calcium [Mass/volume] in Serum or Plasma |
| Lab | 2028-9 Carbon dioxide, total [Moles/volume] in Serum or Plasma |
| Lab | 9318-7 Albumin/Creatinine [Mass Ratio] in Urine |
| Lab | 2777-1 Phosphate [Mass/volume] in Serum or Plasma |
| Lab | 3094-0 Urea nitrogen [Mass/volume] in Serum or Plasma |
| Lab | 2075-0 Chloride [Moles/volume] in Serum or Plasma |
| Lab | 4544-3 Hematocrit [Volume Fraction] of Blood by Automated count |
| Lab | 718-7 Hemoglobin [Mass/volume] in Blood |
| Lab | 2823-3 Potassium [Moles/volume] in Serum or Plasma |
| Drug class | BETA-ADRENERGIC BLOCKING AGENTS |
| Drug class | LOOP DIURETICS |
| Drug class | HMG-COA REDUCTASE INHIBITORS |
| Drug class | DIHYDROPYRIDINES |
| Drug class | ANGIOTENSIN-CONVERTING ENZYME INHIBITORS |
| Drug class | ANGIOTENSIN II RECEPTOR ANTAGONISTS |
| Drug class | VITAMIN D |
| Drug class | DIRECT VASODILATORS |
| Drug class | THIAZIDE DIURETICS |
| Drug class | CHOLESTEROL ABSORPTION INHIBITORS |
| Drug class | THIAZIDE-LIKE DIURETICS |
| Drug class | PHOSPHATE-REMOVING AGENTS |
| Drug class | CENTRAL ALPHA-AGONISTS |
| Drug class | HEMATOPOIETIC AGENTS |
| Drug class | ALPHA-ADRENERGIC BLOCKING AGENTS |
| Diagnosis | 403.11 Ben hyp kid w cr kid V |
| Diagnosis | 403.91 Hyp kid NOS w cr kid V |
| Diagnosis | 285.21 Anemia in chr kidney dis |
| Diagnosis | 588.81 Sec hyperparathyrd-renal |
| Diagnosis | V72.81 Preop cardiovsclr exam |
| Diagnosis | 786.50 Chest pain NOS |
| Diagnosis | 600.00 BPH w/o urinary obs/LUTS |
| Diagnosis | 244.9 Hypothyroidism NOS |
| Diagnosis | 599.0 Urin tract infection NOS |
| Diagnosis | 250.02 DMII wo cmp uncntrld |
| Diagnosis | 250.01 DMI wo cmp nt st uncntrl |
| Diagnosis | 530.81 Esophageal reflux |
| Diagnosis | V58.61 Long-term use anticoagul |
| Diagnosis | 780.79 Malaise and fatigue NEC |
| Diagnosis | 562.10 Dvrtclo colon w/o hmrhg |

Table 4: Area Under ROC curve for comparing the held out test score

| | AUC |
|---|---|
| CNN2 | 0.774 |
| Random forest | 0.774 |
| L1-regularized logistic regression with hand-engineered features | 0.768 |
| L2-regularized logistic regression | 0.755 |

Table 5: Top Features from the baseline model for 585.6 End stage renal disease

| Feature | weight | Feature | weight |
|---|---|---|---|
| Glucose(2345-7) -decreasing | -1.099 | Alanine(1742-6) -increasing | 0.2263 |
| Chloride(2075-0) -latest value | 0.4988 | Cholesterol.in(13457-7) -increasing | -0.216 |
| Glucose(2345-7) -latest value | -0.485 | Urea(3094-0) -maximum | -0.214 |
| Creatinine(2160-0) -maximum | 0.4837 | Aspartate(1920-8) -maximum | 0.2016 |
| Carbon(2028-9) -increasing | 0.4500 | Sodium(2951-2) -latest value | -0.191 |
| Cholesterol.in(13457-7) -minimum | 0.3037 | Creatinine(2160-0) -decreasing | 0.1918 |
| Cholesterol.in(13457-7) -latest value | -0.254 | Chloride(2075-0) -maximum | -0.177 |
| Glucose(2345-7) -minimum | -0.251 | Carbon(2028-9) -minimum | -0.170 |
| Calcium(17861-6) -decreasing | -0.239 | Alanine(1742-6) -minimum | -0.122 |
| Urea(3094-0) -increasing | 0.2344 | Protein(2885-2) -increasing | 0.1208 |

Table 6: Top Features from the baseline model for 285.21 Anemia in chr kidney dis

| Feature | weight | Feature | weight |
|---|---|---|---|
| Chloride(2075-0) -latest value | 0.7909 | Calcium(17861-6) -maximum | -0.305 |
| Cholesterol.in(13457-7) -minimum | 0.7244 | Triglyceride(2571-8) -decreasing | -0.301 |
| Glucose(2345-7) -decreasing | -0.717 | Triglyceride(2571-8) -increasing | -0.300 |
| Creatinine(2160-0) -maximum | 0.5596 | Carbon(2028-9) -maximum | -0.291 |
| Creatinine(2160-0) -minimum | 0.4692 | Cholesterol.in(13457-7) -increasing | -0.290 |
| Chloride(2075-0) -increasing | -0.442 | Alanine(1742-6) -minimum | -0.284 |
| Potassium(2823-3) -increasing | -0.381 | Glucose(2345-7) -latest value | -0.273 |
| Cholesterol.in(13457-7) -latest value | -0.370 | Alanine(1742-6) -increasing | 0.2531 |
| Aspartate(1920-8) -decreasing | 0.3658 | Carbon(2028-9) -increasing | 0.2383 |
| Glucose(2345-7) -minimum | -0.324 | Urea(3094-0) -increasing | 0.2359 |

Table 7: Top Features from the baseline model for 585.3 Chr kidney dis stage III

| Feature | weight | Feature | weight |
|---|---|---|---|
| Glucose(2345-7) -decreasing | -0.749 | Triglyceride(2571-8) -maximum | 0.2169 |
| Cholesterol.in(13457-7) -minimum | 0.6567 | Alanine(1742-6) -maximum | 0.2060 |
| Chloride(2075-0) -latest value | 0.5660 | Cholesterol.in(13457-7) -increasing | -0.200 |
| Triglyceride(2571-8) -increasing | -0.425 | Potassium(2823-3) -decreasing | 0.1638 |
| Creatinine(2160-0) -maximum | 0.4086 | Carbon(2028-9) -increasing | 0.1509 |
| Cholesterol.in(13457-7) -latest value | -0.374 | Alanine(1742-6) -minimum | -0.143 |
| Chloride(2075-0) -maximum | -0.361 | Glucose(2345-7) -minimum | -0.140 |
| Creatinine(2160-0) -minimum | 0.3368 | Calcium(17861-6) -increasing | 0.1407 |
| Glucose(2345-7) -latest value | -0.286 | Albumin(1751-7) -minimum | 0.1385 |
| Alanine(1742-6) -increasing | 0.2667 | Potassium(2823-3) -minimum | -0.137 |

Table 8: Top Features from the baseline model for 584.9 Acute kidney failure NOS

| Feature | weight | Feature | weight |
|---|---|---|---|
| Glucose(2345-7) -decreasing | -0.729 | Carbon(2028-9) -increasing | 0.1915 |
| Creatinine(2160-0) -minimum | 0.3994 | Alanine(1742-6) -minimum | -0.180 |
| Glucose(2345-7) -latest value | -0.388 | Alanine(1742-6) -increasing | 0.1694 |
| Cholesterol.in(13457-7) -latest value | -0.372 | Triglyceride(2571-8) -increasing | -0.156 |
| Creatinine(2160-0) -maximum | 0.3195 | Glucose(2345-7) -maximum | 0.1402 |
| Chloride(2075-0) -latest value | 0.3087 | Potassium(2823-3) -minimum | -0.136 |
| Creatinine(2160-0) -decreasing | 0.2750 | Chloride(2075-0) -increasing | -0.129 |
| Cholesterol.in(13457-7) -minimum | 0.2571 | Aspartate(1920-8) -latest value | 0.1212 |
| Urea(3094-0) -increasing | 0.2374 | Potassium(2823-3) -latest value | 0.1078 |
| Albumin(1751-7) -maximum | 0.2309 | Cholesterol.in(13457-7) -increasing | -0.105 |

Table 9: Top Features from the baseline model for 250.01 DMI wo cmp nt st uncntrl

| Feature | weight | Feature | weight |
|---|---|---|---|
| Alanine(1742-6) -minimum | -0.683 | Creatinine(2160-0) -minimum | 0.1255 |
| Creatinine(2160-0) -decreasing | 0.6438 | Bilirubin(1975-2) -maximum | 0.1244 |
| Glucose(2345-7) -decreasing | -0.235 | Aspartate(1920-8) -increasing | -0.116 |
| Glucose(2345-7) -minimum | -0.227 | Cholesterol(2093-3) -latest value | 0.1157 |
| Urea(3094-0) -decreasing | 0.2204 | Alanine(1742-6) -decreasing | -0.092 |
| Sodium(2951-2) -increasing | 0.1755 | Urea(3097-3) -latest value | -0.078 |
| Urea(3094-0) -increasing | -0.172 | Protein(2885-2) -minimum | 0.0750 |
| Protein(2885-2) -increasing | 0.1526 | Protein(2885-2) -decreasing | -0.072 |
| Albumin(1751-7) -maximum | 0.1274 | Alanine(1742-6) -latest value | 0.0699 |
| Alanine(1742-6) -maximum | -0.126 | Cholesterol.in(13457-7) -increasing | 0.0661 |

Table 10: Top Features from the baseline model for 250.02 DMII wo cmp uncntrld

| Feature | weight | Feature | weight |
|---|---|---|---|
| Alanine(1742-6) -minimum | -0.727 | Urea(3094-0) -minimum | -0.165 |
| Creatinine(2160-0) -decreasing | 0.6069 | Aspartate(1920-8) -maximum | 0.1647 |
| Cholesterol(2093-3) -latest value | 0.3880 | Albumin(1751-7) -maximum | 0.1594 |
| Sodium(2951-2) -increasing | 0.3318 | Protein(2885-2) -increasing | 0.1521 |
| Alanine(1742-6) -increasing | -0.330 | Calcium(17861-6) -increasing | -0.146 |
| Urea(3094-0) -decreasing | 0.2875 | Triglyceride(2571-8) -increasing | -0.145 |
| Glucose(2345-7) -maximum | 0.2016 | Albumin(1751-7) -minimum | 0.1437 |
| Potassium(2823-3) -latest value | -0.184 | Cholesterol.in(13457-7) -minimum | 0.1392 |
| Glucose(2345-7) -decreasing | -0.182 | Creatinine(2160-0) -latest value | -0.136 |
| Aspartate(1920-8) -decreasing | -0.168 | Alanine(1742-6) -maximum | -0.136 |

Table 11: Top Features from the baseline model for 593.9 Renal and ureteral dis NOS

| Feature | weight | Feature | weight |
|---|---|---|---|
| Glucose(2345-7) -decreasing | -0.769 | Urea(3094-0) -maximum | -0.171 |
| Chloride(2075-0) -latest value | 0.5136 | Cholesterol.in(13457-7) -increasing | -0.150 |
| Cholesterol.in(13457-7) -minimum | 0.4754 | Calcium(17861-6) -decreasing | 0.1446 |
| Cholesterol.in(13457-7) -latest value | -0.345 | Alanine(1742-6) -decreasing | -0.143 |
| Alanine(1742-6) -maximum | 0.2568 | Sodium(2951-2) -decreasing | -0.142 |
| Creatinine(2160-0) -maximum | 0.2394 | Carbon(2028-9) -minimum | -0.137 |
| Creatinine(2160-0) -minimum | 0.2163 | Cholesterol.in(13457-7) -decreasing | -0.133 |
| Creatinine(2160-0) -decreasing | 0.2093 | Carbon(2028-9) -increasing | 0.1204 |
| Calcium(17861-6) -maximum | -0.182 | Albumin(1751-7) -maximum | 0.1146 |
| Glucose(2345-7) -maximum | 0.1816 | Alanine(1742-6) -minimum | -0.113 |

Table 12: Top Features from the baseline model for 428.0 CHF NOS

| Feature | weight | Feature | weight |
|---|---|---|---|
| Glucose(2345-7) -decreasing | -0.449 | Alanine(1742-6) -increasing | 0.1467 |
| Glucose(2345-7) -maximum | 0.2493 | Chloride(2075-0) -decreasing | -0.146 |
| Cholesterol.in(13457-7) -minimum | 0.2140 | Creatinine(2160-0) -maximum | 0.1251 |
| Creatinine(2160-0) -decreasing | 0.2126 | Alanine(1742-6) -minimum | -0.124 |
| Albumin(1751-7) -maximum | 0.2045 | Creatinine(2160-0) -latest value | -0.120 |
| Chloride(2075-0) -latest value | 0.1996 | Albumin(1751-7) -latest value | -0.112 |
| Glucose(2345-7) -latest value | -0.195 | Aspartate(1920-8) -decreasing | 0.1106 |
| Creatinine(2160-0) -minimum | 0.1911 | Cholesterol(2093-3) -decreasing | -0.100 |
| Calcium(17861-6) -decreasing | 0.1588 | Alanine(1742-6) -decreasing | 0.1000 |
| Cholesterol.in(13457-7) -maximum | -0.156 | Alanine(1742-6) -latest value | -0.098 |

Table 13: Top Features from the baseline model for V05.3 Need prphyl vc vrl hepat

| Feature | weight | Feature | weight |
|---|---|---|---|
| Carbon(2028-9) -increasing | 0.4567 | Sodium(2951-2) -latest value | 0.0 |
| Creatinine(2160-0) -maximum | 0.4441 | Sodium(2951-2) -decreasing | 0.0 |
| Glucose(2345-7) -decreasing | -0.233 | Sodium(2951-2) -increasing | 0.0 |
| Aspartate(1920-8) -decreasing | 0.1593 | Sodium(2951-2) -minimum | 0.0 |
| Creatinine(2160-0) -minimum | -0.119 | Calcium(17861-6) -decreasing | 0.0 |
| Urea(3094-0) -minimum | -0.109 | Calcium(17861-6) -latest value | 0.0 |
| Creatinine(2160-0) -increasing | -0.058 | Calcium(17861-6) -increasing | 0.0 |
| Protein(2885-2) -maximum | 0.0177 | Calcium(17861-6) -minimum | 0.0 |
| Alanine(1742-6) -maximum | 0.0164 | Calcium(17861-6) -maximum | 0.0 |
| Chloride(2075-0) -maximum | 0.0 | Cholesterol.in(13457-7) -latest value | 0.0 |

Table 14: Top Features from the baseline model for 790.93 Elvtd prstate spcf antgn

| Feature | weight | Feature | weight |
|---|---|---|---|
| Alanine(1742-6) -maximum | 0.2819 | Triglyceride(2571-8) -minimum | 0.1261 |
| Potassium(2823-3) -minimum | 0.2446 | Alanine(1742-6) -increasing | -0.120 |
| Sodium(2951-2) -latest value | 0.2335 | Protein(2885-2) -increasing | -0.115 |
| Cholesterol.in(13457-7) -minimum | 0.2137 | Triglyceride(2571-8) -increasing | -0.096 |
| Creatinine(2160-0) -decreasing | -0.179 | Alanine(1742-6) -decreasing | 0.0861 |
| Cholesterol(2093-3) -latest value | 0.1770 | Sodium(2951-2) -increasing | 0.0832 |
| Potassium(2823-3) -increasing | -0.146 | Urea(3097-3) -latest value | 0.0789 |
| Glucose(2345-7) -minimum | 0.1437 | Potassium(2823-3) -decreasing | -0.076 |
| Cholesterol(2093-3) -maximum | -0.138 | Albumin(1751-7) -decreasing | -0.073 |
| Cholesterol(2093-3) -increasing | 0.1277 | Cholesterol(2093-3) -minimum | -0.070 |

Table 15: Top Features from the baseline model for 185. Malign neopl prostate

| Feature | weight | Feature | weight |
|---|---|---|---|
| Cholesterol(2093-3) -minimum | -0.293 | Cholesterol(2093-3) -latest value | 0.1599 |
| Aspartate(1920-8) -maximum | 0.2527 | Sodium(2951-2) -decreasing | 0.1498 |
| Alanine(1742-6) -latest value | 0.2005 | Cholesterol(2093-3) -maximum | -0.144 |
| Glucose(2345-7) -decreasing | -0.188 | Triglyceride(2571-8) -minimum | 0.1375 |
| Cholesterol.in(13457-7) -minimum | 0.1791 | Cholesterol(2093-3) -increasing | 0.1334 |
| Aspartate(1920-8) -decreasing | -0.174 | Alanine(1742-6) -decreasing | -0.130 |
| Alanine(1742-6) -increasing | -0.173 | Potassium(2823-3) -minimum | 0.1305 |
| Potassium(2823-3) -decreasing | -0.168 | Potassium(2823-3) -maximum | 0.1143 |
| Alanine(1742-6) -maximum | 0.1676 | Urea(3094-0) -maximum | -0.110 |
| Sodium(2951-2) -increasing | 0.1648 | Bilirubin(1975-2) -decreasing | -0.108 |

Table 16: Top Features from the baseline model for 274.9 Gout NOS

| Feature | weight | Feature | weight |
|---|---|---|---|
| Glucose(2345-7) -decreasing | -0.414 | Creatinine(2160-0) -decreasing | 0.1201 |
| Cholesterol.in(13457-7) -latest value | -0.266 | Urea(3094-0) -increasing | 0.1181 |
| Aspartate(1920-8) -increasing | -0.261 | Carbon(2028-9) -increasing | 0.1005 |
| Cholesterol.in(13457-7) -minimum | 0.2584 | Aspartate(1920-8) -maximum | 0.0980 |
| Creatinine(2160-0) -maximum | 0.2092 | Protein(2885-2) -decreasing | -0.096 |
| Glucose(2345-7) -latest value | -0.200 | Chloride(2075-0) -latest value | 0.0953 |
| Glucose(2345-7) -increasing | -0.194 | Creatinine(2160-0) -minimum | 0.0881 |
| Urea(3094-0) -minimum | 0.1545 | Creatinine(2160-0) -latest value | -0.086 |
| Alanine(1742-6) -maximum | 0.1316 | Aspartate(1920-8) -latest value | -0.078 |
| Protein(2885-2) -latest value | 0.1295 | Cholesterol(2093-3) -increasing | -0.077 |

Table 17: Top Features from the baseline model for 362.52 Exudative macular degen

| Feature | weight | Feature | weight |
|---|---|---|---|
| Creatinine(2160-0) -maximum | 0.3761 | Glucose(2345-7) -decreasing | 0.1683 |
| Creatinine(2160-0) -latest value | -0.270 | Creatinine(2160-0) -minimum | 0.1545 |
| Alanine(1742-6) -latest value | -0.254 | Cholesterol.in(13457-7) -increasing | 0.1477 |
| Urea(3094-0) -increasing | -0.241 | Albumin(1751-7) -latest value | -0.145 |
| Alanine(1742-6) -increasing | 0.2399 | Potassium(2823-3) -latest value | 0.1365 |
| Alanine(1742-6) -minimum | 0.2304 | Aspartate(1920-8) -increasing | -0.120 |
| Glucose(2345-7) -latest value | -0.200 | Calcium(17861-6) -decreasing | 0.1134 |
| Potassium(2823-3) -minimum | 0.1818 | Glucose(2345-7) -minimum | 0.0982 |
| Cholesterol.in(13457-7) -latest value | 0.1795 | Aspartate(1920-8) -minimum | 0.0966 |
| Urea(3094-0) -maximum | -0.168 | Carbon(2028-9) -increasing | -0.090 |

Table 18: Top Features from the baseline model for 607.84 Impotence, organic orign

| Feature | weight | Feature | weight |
|---|---|---|---|
| Cholesterol(2093-3) -minimum | -0.296 | Urea(3094-0) -increasing | -0.140 |
| Alanine(1742-6) -maximum | 0.2400 | Glucose(2345-7) -latest value | 0.1306 |
| Alanine(1742-6) -increasing | -0.237 | Aspartate(1920-8) -decreasing | -0.116 |
| Aspartate(1920-8) -increasing | -0.210 | Urea(3094-0) -minimum | -0.111 |
| Potassium(2823-3) -increasing | 0.1967 | Protein(2885-2) -maximum | 0.1038 |
| Potassium(2823-3) -decreasing | 0.1671 | Chloride(2075-0) -minimum | 0.0963 |
| Creatinine(2160-0) -maximum | -0.160 | Cholesterol.in(13457-7) -minimum | 0.0905 |
| Protein(2885-2) -latest value | -0.153 | Creatinine(2160-0) -increasing | -0.086 |
| Creatinine(2160-0) -decreasing | 0.1531 | Aspartate(1920-8) -latest value | 0.0856 |
| Calcium(17861-6) -latest value | -0.141 | Alanine(1742-6) -decreasing | -0.078 |

Table 19: Top Features from the baseline model for 511.9 Pleural effusion NOS

| Feature | weight | Feature | weight |
|---|---|---|---|
| Alanine(1742-6) -increasing | 0.4040 | Triglyceride(2571-8) -increasing | -0.194 |
| Glucose(2345-7) -decreasing | -0.366 | Creatinine(2160-0) -maximum | 0.1678 |
| Urea(3094-0) -latest value | -0.297 | Aspartate(1920-8) -increasing | -0.166 |
| Chloride(2075-0) -latest value | 0.2698 | Cholesterol.in(13457-7) -decreasing | -0.158 |
| Urea(3094-0) -increasing | 0.2680 | Glucose(2345-7) -latest value | -0.154 |
| Chloride(2075-0) -maximum | -0.251 | Cholesterol(2093-3) -decreasing | -0.154 |
| Aspartate(1920-8) -latest value | 0.2400 | Creatinine(2160-0) -latest value | 0.1370 |
| Cholesterol.in(13457-7) -minimum | 0.2396 | Cholesterol.in(13457-7) -maximum | -0.135 |
| Alanine(1742-6) -minimum | -0.223 | Albumin(1751-7) -maximum | 0.1317 |
| Alanine(1742-6) -maximum | -0.200 | Triglyceride(2571-8) -maximum | -0.129 |

Table 20: Top Features from the baseline model for 616.10 Vaginitis NOS

| Feature | weight | Feature | weight |
|---|---|---|---|
| Alanine(1742-6) -maximum | -0.567 | Cholesterol(2093-3) -maximum | 0.1796 |
| Protein(2885-2) -decreasing | -0.386 | Creatinine(2160-0) -maximum | -0.172 |
| Alanine(1742-6) -increasing | 0.3732 | Cholesterol.in(13457-7) -minimum | -0.151 |
| Creatinine(2160-0) -increasing | -0.340 | Calcium(17861-6) -decreasing | 0.1461 |
| Calcium(17861-6) -maximum | 0.2638 | Triglyceride(2571-8) -increasing | 0.0902 |
| Urea(3094-0) -latest value | -0.263 | Bilirubin(1975-2) -minimum | -0.075 |
| Creatinine(2160-0) -minimum | -0.230 | Albumin/Globulin(1759-0) -increasing | 0.0708 |
| Protein(2885-2) -minimum | -0.200 | Urea(3094-0) -increasing | -0.067 |
| Cholesterol.in(13457-7) -latest value | 0.1909 | Glucose(2345-7) -decreasing | 0.0619 |
| Glucose(2345-7) -minimum | -0.190 | Potassium(2823-3) -decreasing | -0.058 |

Table 21: Top Features from the baseline model for 600.01 BPH w urinary obs/LUTS

| Feature | weight | Feature | weight |
|---|---|---|---|
| Glucose(2345-7) -decreasing | -0.358 | Sodium(2951-2) -latest value | 0.1253 |
| Alanine(1742-6) -increasing | -0.324 | Chloride(2075-0) -latest value | 0.1236 |
| Creatinine(2160-0) -latest value | -0.255 | Cholesterol.in(13457-7) -decreasing | -0.114 |
| Protein(2885-2) -latest value | -0.253 | Aspartate(1920-8) -increasing | -0.100 |
| Sodium(2951-2) -decreasing | 0.2298 | Creatinine(2160-0) -decreasing | 0.0918 |
| Cholesterol.in(13457-7) -minimum | 0.1959 | Cholesterol.in(13457-7) -latest value | -0.091 |
| Aspartate(1920-8) -maximum | 0.1736 | Chloride(2075-0) -increasing | -0.083 |
| Glucose(2345-7) -increasing | -0.134 | Urea(3094-0) -maximum | -0.076 |
| Creatinine(2160-0) -maximum | -0.133 | Potassium(2823-3) -increasing | -0.072 |
| Urea(3094-0) -latest value | 0.1271 | Chloride(2075-0) -decreasing | -0.071 |

Table 22: Top Features from the baseline model for 285.29 Anemia-other chronic dis

| Feature | weight | Feature | weight |
|---|---|---|---|
| Glucose(2345-7) -decreasing | -0.492 | Triglyceride(2571-8) -increasing | -0.205 |
| Creatinine(2160-0) -increasing | 0.3508 | Urea(3094-0) -maximum | -0.189 |
| Protein(2885-2) -latest value | 0.3098 | Albumin(1751-7) -maximum | 0.1885 |
| Aspartate(1920-8) -decreasing | 0.3042 | Aspartate(1920-8) -maximum | -0.183 |
| Carbon(2028-9) -increasing | 0.2610 | Chloride(2075-0) -latest value | 0.1796 |
| Creatinine(2160-0) -maximum | 0.2594 | Potassium(2823-3) -latest value | -0.168 |
| Alanine(1742-6) -increasing | 0.2468 | Aspartate(1920-8) -latest value | 0.1632 |
| Creatinine(2160-0) -minimum | 0.2386 | Creatinine(2160-0) -decreasing | 0.1492 |
| Potassium(2823-3) -minimum | 0.2368 | Cholesterol.in(13457-7) -decreasing | -0.147 |
| Cholesterol.in(13457-7) -increasing | -0.216 | Cholesterol(2093-3) -latest value | -0.134 |

Table 23: Top Features from the baseline model for 346.90 Migrne unsp wo ntrc mgrn

| Feature | weight | Feature | weight |
|---|---|---|---|
| Cholesterol.in(13457-7) -minimum | -0.403 | Aspartate(1920-8) -maximum | -0.105 |
| Cholesterol(2093-3) -increasing | 0.3081 | Alanine(1742-6) -latest value | -0.102 |
| Cholesterol.in(13457-7) -latest value | 0.2965 | Creatinine(2160-0) -increasing | -0.096 |
| Alanine(1742-6) -minimum | 0.2748 | Protein(2885-2) -decreasing | 0.0964 |
| Sodium(2951-2) -decreasing | -0.204 | Sodium(2951-2) -minimum | 0.0925 |
| Cholesterol.in(13457-7) -decreasing | 0.1985 | Potassium(2823-3) -latest value | -0.088 |
| Aspartate(1920-8) -increasing | 0.1974 | Potassium(2823-3) -decreasing | -0.084 |
| Albumin/Globulin(1759-0) -increasing | 0.1783 | Carbon(2028-9) -maximum | 0.0836 |
| Glucose(2345-7) -latest value | -0.132 | Albumin/Globulin(1759-0) -maximum | 0.0587 |
| Protein(2885-2) -maximum | 0.1100 | Calcium(17861-6) -decreasing | 0.0528 |

Table 24: Top Features from the baseline model for 427.31 Atrial fibrillation

| Feature | weight | Feature | weight |
|---|---|---|---|
| Creatinine(2160-0) -maximum | 0.2260 | Albumin/Globulin(1759-0) -latest value | -0.019 |
| Alanine(1742-6) -increasing | 0.1981 | Creatinine(2160-0) -latest value | -0.015 |
| Glucose(2345-7) -maximum | 0.1956 | Urea(3097-3) -latest value | -0.011 |
| Glucose(2345-7) -latest value | -0.099 | Sodium(2951-2) -decreasing | 0.0089 |
| Urea(3094-0) -maximum | -0.089 | Creatinine(2160-0) -minimum | 0.0084 |
| Urea(3094-0) -latest value | -0.082 | Cholesterol.in(13457-7) -latest value | -0.007 |
| Glucose(2345-7) -decreasing | -0.079 | Cholesterol(2093-3) -decreasing | -0.000 |
| Alanine(1742-6) -minimum | -0.066 | Potassium(2823-3) -minimum | 0.0 |
| Urea(3094-0) -minimum | -0.037 | Chloride(2075-0) -minimum | 0.0 |
| Cholesterol(2093-3) -increasing | -0.031 | Chloride(2075-0) -maximum | 0.0 |

Table 25: Top Features from the baseline model for 250.00 DMII wo cmp nt st uncntr

| Feature | weight | Feature | weight |
|---|---|---|---|
| Alanine(1742-6) -minimum | -0.406 | Sodium(2951-2) -maximum | -0.104 |
| Aspartate(1920-8) -increasing | -0.371 | Potassium(2823-3) -latest value | -0.099 |
| Creatinine(2160-0) -decreasing | 0.2839 | Urea(3097-3) -maximum | 0.0990 |
| Albumin(1751-7) -maximum | 0.2038 | Triglyceride(2571-8) -maximum | 0.0983 |
| Alanine(1742-6) -increasing | -0.184 | Urea(3094-0) -decreasing | 0.0894 |
| Glucose(2345-7) -maximum | 0.1364 | Cholesterol.in(13457-7) -minimum | 0.0803 |
| Aspartate(1920-8) -maximum | 0.1264 | Chloride(2075-0) -increasing | -0.075 |
| Cholesterol.in(13457-7) -latest value | 0.1119 | Aspartate(1920-8) -minimum | 0.0737 |
| Calcium(17861-6) -increasing | -0.107 | Glucose(2345-7) -increasing | 0.0639 |
| Glucose(2345-7) -decreasing | -0.105 | Bilirubin(1975-2) -increasing | -0.060 |

Table 26: Top Features from the baseline model for 425.4 Prim cardiomyopathy NEC

| Feature | weight | Feature | weight |
|---|---|---|---|
| Glucose(2345-7) -decreasing | -0.272 | Urea(3094-0) -increasing | -0.010 |
| Creatinine(2160-0) -maximum | 0.1168 | Protein(2885-2) -latest value | 0.0038 |
| Albumin(1751-7) -maximum | 0.1132 | Sodium(2951-2) -latest value | 0.0 |
| Urea(3094-0) -latest value | -0.070 | Chloride(2075-0) -maximum | 0.0 |
| Creatinine(2160-0) -minimum | 0.0647 | Chloride(2075-0) -minimum | 0.0 |
| Creatinine(2160-0) -decreasing | 0.0560 | Sodium(2951-2) -decreasing | 0.0 |
| Urea(3094-0) -maximum | -0.025 | Sodium(2951-2) -increasing | 0.0 |
| Glucose(2345-7) -maximum | 0.0167 | Sodium(2951-2) -maximum | 0.0 |
| Aspartate(1920-8) -maximum | 0.0165 | Chloride(2075-0) -increasing | 0.0 |
| Glucose(2345-7) -latest value | -0.014 | Calcium(17861-6) -latest value | 0.0 |

Table 27: Top Features from the baseline model for 728.87 Muscle weakness-general

| Feature | weight | Feature | weight |
|---|---|---|---|
| Alanine(1742-6) -increasing | 0.2943 | Glucose(2345-7) -latest value | -0.087 |
| Creatinine(2160-0) -minimum | 0.2361 | Calcium(17861-6) -latest value | -0.083 |
| Glucose(2345-7) -decreasing | -0.189 | Calcium(17861-6) -maximum | -0.079 |
| Creatinine(2160-0) -decreasing | 0.1719 | Urea(3094-0) -latest value | -0.076 |
| Creatinine(2160-0) -increasing | 0.1644 | Alanine(1742-6) -maximum | -0.075 |
| Creatinine(2160-0) -maximum | 0.1479 | Alanine(1742-6) -latest value | -0.071 |
| Alanine(1742-6) -minimum | -0.112 | Albumin(1751-7) -minimum | 0.0697 |
| Triglyceride(2571-8) -maximum | -0.108 | Cholesterol.in(13457-7) -increasing | -0.067 |
| Urea(3094-0) -minimum | 0.1040 | Protein(2885-2) -decreasing | -0.064 |
| Aspartate(1920-8) -minimum | 0.1020 | Protein(2885-2) -increasing | 0.0623 |

Table 28: Top Features from the baseline model for 620.2 Ovarian cyst NEC/NOS

| Feature | weight | Feature | weight |
|---|---|---|---|
| Alanine(1742-6) -decreasing | 0.5072 | Protein(2885-2) -decreasing | 0.1532 |
| Cholesterol.in(13457-7) -minimum | -0.287 | Urea(3094-0) -minimum | -0.147 |
| Aspartate(1920-8) -decreasing | -0.285 | Cholesterol.in(13457-7) -increasing | -0.136 |
| Alanine(1742-6) -latest value | -0.232 | Alanine(1742-6) -maximum | -0.131 |
| Urea(3094-0) -decreasing | -0.213 | Glucose(2345-7) -decreasing | 0.1079 |
| Creatinine(2160-0) -latest value | 0.2003 | Aspartate(1920-8) -latest value | 0.1043 |
| Chloride(2075-0) -maximum | 0.1717 | Glucose(2345-7) -minimum | 0.1004 |
| Urea(3094-0) -maximum | 0.1681 | Albumin(1751-7) -maximum | 0.0953 |
| Creatinine(2160-0) -maximum | -0.157 | Urea(3097-3) -latest value | 0.0884 |
| Glucose(2345-7) -increasing | -0.156 | Albumin(1751-7) -latest value | 0.0792 |

Table 29: Top Features from the baseline model for 286.9 Coagulat defect NEC/NOS

| Feature | weight | Feature | weight |
|---|---|---|---|
| Chloride(2075-0) -minimum | -0.337 | Creatinine(2160-0) -maximum | 0.1148 |
| Carbon(2028-9) -increasing | 0.3219 | Glucose(2345-7) -maximum | 0.1124 |
| Glucose(2345-7) -decreasing | -0.300 | Creatinine(2160-0) -latest value | 0.1008 |
| Creatinine(2160-0) -minimum | 0.2578 | Aspartate(1920-8) -decreasing | 0.0993 |
| Triglyceride(2571-8) -increasing | -0.203 | Albumin(1751-7) -latest value | -0.090 |
| Albumin(1751-7) -maximum | 0.1802 | Creatinine(2160-0) -increasing | 0.0865 |
| Alanine(1742-6) -minimum | -0.179 | Sodium(2951-2) -maximum | -0.082 |
| Cholesterol(2093-3) -latest value | -0.147 | Urea(3097-3) -latest value | -0.080 |
| Protein(2885-2) -decreasing | -0.139 | Alanine(1742-6) -increasing | 0.0764 |
| Triglyceride(2571-8) -latest value | -0.123 | Potassium(2823-3) -latest value | -0.075 |

Table 30: Top Features from the baseline model for 443.9 Periph vascular dis NOS

| Feature | weight | Feature | weight |
|---|---|---|---|
| Glucose(2345-7) -decreasing | -0.395 | Creatinine(2160-0) -maximum | 0.1184 |
| Alanine(1742-6) -increasing | 0.2594 | Triglyceride(2571-8) -minimum | 0.1182 |
| Alanine(1742-6) -minimum | -0.227 | Triglyceride(2571-8) -increasing | -0.116 |
| Cholesterol.in(13457-7) -latest value | -0.199 | Sodium(2951-2) -increasing | 0.1053 |
| Aspartate(1920-8) -latest value | 0.1825 | Chloride(2075-0) -minimum | -0.095 |
| Creatinine(2160-0) -minimum | 0.1554 | Urea(3094-0) -increasing | 0.0914 |
| Glucose(2345-7) -maximum | 0.1403 | Albumin/Globulin(1759-0) -maximum | -0.077 |
| Protein(2885-2) -decreasing | -0.133 | Aspartate(1920-8) -increasing | -0.075 |
| Urea(3094-0) -latest value | -0.128 | Aspartate(1920-8) -minimum | 0.0724 |
| Glucose(2345-7) -minimum | -0.123 | Cholesterol.in(13457-7) -decreasing | -0.065 |

Table 31: Top Features from the baseline model for 362.51 Nonexudat macular degen

| Feature | weight | Feature | weight |
|---|---|---|---|
| Creatinine(2160-0) -latest value | -0.117 | Sodium(2951-2) -decreasing | 0.0 |
| Glucose(2345-7) -decreasing | -0.080 | Sodium(2951-2) -increasing | 0.0 |
| Protein(2885-2) -latest value | -0.060 | Sodium(2951-2) -minimum | 0.0 |
| Creatinine(2160-0) -increasing | 0.0179 | Sodium(2951-2) -maximum | 0.0 |
| Glucose(2345-7) -latest value | -0.015 | Calcium(17861-6) -decreasing | 0.0 |
| Creatinine(2160-0) -maximum | 0.0099 | Chloride(2075-0) -minimum | 0.0 |
| Glucose(2345-7) -minimum | 0.0075 | Calcium(17861-6) -increasing | 0.0 |
| Urea(3094-0) -latest value | -0.001 | Calcium(17861-6) -minimum | 0.0 |
| Chloride(2075-0) -maximum | 0.0 | Calcium(17861-6) -maximum | 0.0 |
| Sodium(2951-2) -latest value | 0.0 | Cholesterol.in(13457-7) -latest value | 0.0 |

Table 32: Top Features from the baseline model for 414.9 Chr ischemic hrt dis NOS

| Feature | weight | Feature | weight |
|---|---|---|---|
| Glucose(2345-7) -decreasing | -0.328 | Chloride(2075-0) -latest value | 0.1241 |
| Glucose(2345-7) -maximum | 0.2678 | Alanine(1742-6) -minimum | -0.116 |
| Aspartate(1920-8) -increasing | -0.264 | Sodium(2951-2) -increasing | 0.1142 |
| Cholesterol.in(13457-7) -latest value | -0.229 | Cholesterol.in(13457-7) -increasing | -0.108 |
| Creatinine(2160-0) -decreasing | 0.1837 | Cholesterol(2093-3) -minimum | -0.103 |
| Creatinine(2160-0) -minimum | 0.1787 | Triglyceride(2571-8) -increasing | -0.096 |
| Aspartate(1920-8) -latest value | 0.1648 | Chloride(2075-0) -decreasing | -0.070 |
| Alanine(1742-6) -decreasing | 0.1462 | Urea(3094-0) -maximum | 0.0699 |
| Creatinine(2160-0) -latest value | -0.139 | Calcium(17861-6) -maximum | -0.069 |
| Cholesterol(2093-3) -latest value | 0.1360 | Potassium(2823-3) -decreasing | 0.0680 |

Table 33: Top Features from the baseline model for 781.2 Abnormality of gait

| Feature | weight | Feature | weight |
|---|---|---|---|
| Alanine(1742-6) -increasing | 0.1921 | Cholesterol.in(13457-7) -minimum | 0.1334 |
| Glucose(2345-7) -latest value | -0.180 | Alanine(1742-6) -maximum | -0.128 |
| Creatinine(2160-0) -increasing | 0.1772 | Aspartate(1920-8) -latest value | 0.1276 |
| Triglyceride(2571-8) -increasing | -0.170 | Chloride(2075-0) -latest value | 0.0991 |
| Creatinine(2160-0) -minimum | 0.1568 | Creatinine(2160-0) -latest value | -0.097 |
| Calcium(17861-6) -decreasing | 0.1538 | Aspartate(1920-8) -increasing | 0.0878 |
| Chloride(2075-0) -maximum | -0.148 | Alanine(1742-6) -latest value | -0.081 |
| Creatinine(2160-0) -decreasing | 0.1446 | Cholesterol.in(13457-7) -increasing | -0.077 |
| Creatinine(2160-0) -maximum | 0.1418 | Glucose(2345-7) -decreasing | -0.074 |
| Protein(2885-2) -decreasing | -0.141 | Potassium(2823-3) -latest value | -0.069 |

Table 34: Top Features from the baseline model for 280.9 Iron defic anemia NOS

| Feature | weight | Feature | weight |
|---|---|---|---|
| Glucose(2345-7) -decreasing | -0.360 | Urea(3094-0) -minimum | 0.1416 |
| Urea(3094-0) -increasing | 0.2385 | Triglyceride(2571-8) -minimum | -0.141 |
| Carbon(2028-9) -increasing | 0.2151 | Protein(2885-2) -minimum | -0.127 |
| Cholesterol.in(13457-7) -latest value | -0.208 | Carbon(2028-9) -maximum | -0.125 |
| Cholesterol.in(13457-7) -increasing | -0.205 | Creatinine(2160-0) -minimum | 0.1219 |
| Aspartate(1920-8) -decreasing | 0.1938 | Aspartate(1920-8) -increasing | 0.1147 |
| Creatinine(2160-0) -increasing | 0.1650 | Protein(2885-2) -latest value | 0.1064 |
| Alanine(1742-6) -increasing | 0.1560 | Potassium(2823-3) -maximum | 0.1056 |
| Chloride(2075-0) -latest value | 0.1500 | Urea(3097-3) -minimum | -0.097 |
| Creatinine(2160-0) -decreasing | 0.1487 | Creatinine(2160-0) -maximum | 0.0954 |